

UCLA

UCLA Previously Published Works

Title

Enzyme-Catalyzed Intramolecular Enantioselective Hydroalkoxylation

Permalink

<https://escholarship.org/uc/item/08m58101>

Journal

Journal of the American Chemical Society, 139(10)

ISSN

0002-7863

Authors

Gao, Shu-Shan
Garcia-Borràs, Marc
Barber, Joyann S
et al.

Publication Date

2017-03-15

DOI

10.1021/jacs.7b01089

Peer reviewed



Published in final edited form as:

J Am Chem Soc. 2017 March 15; 139(10): 3639–3642. doi:10.1021/jacs.7b01089.

Enzyme-Catalyzed Intramolecular Enantioselective Hydroalkoxylation

Shu-Shan Gao[§], Marc Garcia-Borràs[⊥], Joyann S. Barber[⊥], Yang Hai[§], Abing Duan[⊥], Neil K. Garg^{⊥,*}, K. N. Houk^{⊥,*}, and Yi Tang^{*,§,⊥}

[§]Department of Chemical and Biomolecular Engineering, University of California, Los Angeles, California 90095, United States

[⊥]Department of Chemistry and Biochemistry, University of California, Los Angeles, California 90095, United States

Abstract

Hydroalkoxylation is a powerful and efficient method of forming C–O bonds and cyclic ethers in synthetic chemistry. In studying the biosynthesis of the fungal natural product herqueinone, we identified an enzyme that can perform an intramolecular enantio-selective hydroalkoxylation reaction. PhnH catalyzes the addition of a phenol to the terminal olefin of a reverse prenyl group to give a dihydrobenzofuran product. The enzyme accelerates the reaction by 3×10^5 -fold compared to the uncatalyzed reaction. PhnH belongs to a superfamily of proteins with a domain of unknown function (DUF3237), of which no member has a previously verified function. The discovery of PhnH demonstrates that enzymes can be used to promote the enantioselective hydroalkoxylation reaction and form cyclic ethers.

Five- and six-membered cyclic ethers are ubiquitous structural fragments in natural products and are important for their diverse biological activities.¹ Notable examples include the topical antibiotic mupirocin, which contains a tetrahydropyran pharmacophore that binds to the target isoleucyl-tRNA synthetase,^{2a} the anticancer drug eribulin,^{2b} and the antifungal drug griseofulvin.^{2c} Biosynthetically, formation of hydrofurans and hydroxyfurans can proceed via general acid- and general base-catalyzed addition of alcohols to electrophiles such as epoxides, carbonyls, and Michael acceptors (Figure 1A).^{1a} Such reactions are also prevalent in synthetic chemistry.³

*Corresponding Authors: neilgarg@chem.ucla.edu, houk@chem.ucla.edu, yitang@ucla.edu.

ORCID

Yang Hai: 0000-0002-2039-5367

Neil K. Garg: 0000-0002-7793-2629

K. N. Houk: 0000-0002-8387-5261

Yi Tang: 0000-0003-1597-0141

Notes

The authors declare no competing financial interest.

Supporting Information

The Supporting Information is available free of charge on the ACS Publications website at DOI: 10.1021/jacs.7b01089.

Experimental details; spectroscopic and computational data; Tables S1–S8 and Figures S1–S41 (PDF)

An alternative and perhaps more versatile method of forging a new C–O bond involves the hydroalkoxylation of olefins to produce Markovnikov addition products.⁴ The transformation utilizes simple starting materials (i.e., an alcohol and an alkene), is atom economical, and can be used to form two bonds in one step without a change in oxidation state.⁵ Brønsted acid catalysts, such as triflic acid^{6a} and imidazolium or triazolium ionic liquids,^{6b} have been shown to catalyze the nonstereoselective formation of cyclic ethers with very high yields. Regarding enantioselective variants of hydroalkoxylation, several transition-metal-catalyzed reactions have been reported.⁷ However, a dedicated enzyme that can catalyze enantioselective hydroalkoxylation reaction has not been reported, which is surprising given the prevalence of cyclic ether structures found in Nature. One example of enzymatic hydroalkoxylation occurs in the last step of a three-step transformation catalyzed by the monoterpene cyclase 1,8-cineole synthase, proposed to convert the α -terpineol intermediate to 1,8-cineole.⁸ Interestingly, 1,8-cineole synthase cannot convert exogenously added α -terpineol to 1,8-cineole,^{8b,c} which suggests that formation of a tertiary carbocation during the overall terpene cyclization cascade is required for the intramolecular alkylation of the hydroxyl group.^{8c}

Of the cyclic ethers encountered in natural product structures, the dihydrobenzofuran moiety attracted our attention. It is found in the bacterial meroterpenoid neomarinone **1**,⁹ the fungal polyketide herqueinone **2**,¹⁰ and the plant xanthone pruniflorone M **3**¹¹ (Figure 1B), as well as numerous other natural products (see Figure S2). The common structural component present in compounds **1–3** is the 2,3,3-trisubstituted dihydrobenzofuran. The presence of the 3,3-*gem*-dialkyl substitution suggests the dihydrofuran (DHF) ring is formed from the 5-*exo-trig* addition of the phenolic oxygen to the terminal olefin of a reverse prenyl unit, as shown in Figure 1C. Interestingly, all of these natural products are isolated as a single stereoisomer in the DHF rings, suggesting the cyclization step is most likely enzyme-catalyzed. Motivated by the goal of identifying an enzyme that can catalyze hydroalkoxylation, we performed biochemical characterization of the enzymes involved in biosynthesis of **2**. Here we show that an enzyme with a conserved domain of unknown function (DUF) belonging to the DUF3237 superfamily is indeed dedicated to catalyze enantioselective cyclization to form the DHF ring of **2**.

We recently identified the herqueinone (*phn*) biosynthetic gene cluster from *Penicillium herquei* NRRL 1040 (Figure S3) and showed that the actions of a nonreducing polyketide synthase (NR-PKS PhnA) and a flavin-dependent mono-oxygenase (FMO, PhnB) are responsible for formation of phenalenone **5** (Figure 2B).¹² In the process of identifying the unknown steps that lead to formation of the additional DHF ring in **2**, we generated individual knockout mutants of the pathway and characterized the products. Inactivation of the predicted aromatic prenyltransferase PhnF led to abolishment of **2** and accumulation of **5** (Figures 2C-ii and S5), indicating the role of PhnF in catalyzing regioselective C6 alkylation of **5**.

To verify the function of PhnF, the recombinant enzyme (48 kDa) was expressed and purified from *Escherichia coli* BL21-(DE3) (Figure S6). Due to instability of **5**, we assayed using the immediate precursor **4** in the presence of PhnB (with cofactors NADPH and FAD, Figure 2D-i, together with PhnF (with dimethylallyl pyrophosphate (DMAPP)) and MgCl₂,

Figure 2-Dii). Two new products **6a** and **6b** with the same molecular weight (MW = 342) were observed. To scale up the reaction and determine the structures of **6a,b**, we coexpressed PhnA, PhnB, and PhnF in *Saccharomyces cerevisiae* BJ5464-NpgA, which led to the production of **6a,b** (Figure 2C-iv), whereas coexpression of PhnA and PhnB produced only **5** (Figure 2C-iii). During purification, it was observed that **6a,b** are interconverting tautomers; a final ratio of 1:2 of **6a/6b** was found in the purified compound (Figure S13). NMR structural analysis confirmed that **6a** is the C6-reverse prenylated version of **5**, while **6b** is the corresponding diketo tautomer (Figure 2B, Table S1 and Figures S17–S21). When the mixture of **6a,b** was supplemented to the *phnA* blocked mutant of *P. herquei*,¹² the biosynthesis of **2** was restored (Figure S4-iii), confirming the prenylated phenalenone is an authentic intermediate of the pathway, which represents the immediate precursor to the proposed hydroalkoxylation reaction.

The reverse C-prenylation of **5** by PhnF can occur by direct electrophilic substitution at C6, or possibly via first a forward O-prenylation of a neighboring phenol in **5**, followed by a Claisen rearrangement to yield **6**.¹³ Schmidt et al. showed that the forward C-prenylated tyrosine residue in cyanobactins is the product of a nonenzymatic Claisen rearrangement following a reverse O-prenylation catalyzed by the prenyltransferase LynF.¹⁴ However, such rearrangement has not been observed for the prenyltransferases catalyzing forward O-prenylations, such as PagF¹⁵ and SirD.¹⁶ Indeed, density functional theory (DFT) calculations show that Claisen rearrangement after the forward O-prenylation at C7-OH of **5** would be very slow at room temperature ($G^\ddagger_{298} = 30.2$ kcal/mol with predicted $t_{1/2}(25^\circ\text{C}) = 4.2 \times 10^5$ h, Figure S35). Thus, we conclude PhnF must be a reverse C-prenyltransferase that directly alkylates **5**.

We next examined the stability of **6a,b** and whether a spontaneous cyclization of the DHF ring can take place. In phosphate buffer at pH 7.4, rapid degradation of the compounds was observed (Figure S9). In DMSO, ~40% of purified **6** (50 mM starting concentration) was converted to a new compound **8*** in 23 days (Figure S10). The structure of the compounds was determined to contain the racemic DHF ring, as shown in Figure 3A. We propose that **8*** should be derived from the autoxidation of the cyclized product **7***, first as the 1,2,3-triketo intermediate, followed by water addition at C2.¹³ Similarly, **9*** (Table S7 and Figures S30–S33), the acetone adduct of oxidized **7***, was observed when **6** was placed in a 1:1 mixture of acetone/water for 5 days (30% conversion) (Figures 3A and S11). Both **8*** and **9*** displayed optical rotation of $[\alpha]_D = 0$ (c 0.02, MeOH), confirming the uncatalyzed hydroalkoxylation reaction is non-stereospecific. This observation, together with the slow rate of uncatalyzed reaction, indicates an additional enzyme in the *phn* pathway is required to catalyze formation of the 2'-*R*-DHF in **2**.

To search for the enzyme responsible, we performed combinatorial expression of the remaining *phn* enzymes in *S. cerevisiae* (Table S2). None of remaining enzymes in the cluster produced new compounds (Figure S7). RT-PCR of genes immediately outside the initial cluster boundary revealed that only one gene is cotranscribed with the *phn* cluster (Figure S8). This gene, named *phnH*, encodes a small protein (149 aa) that contains a conserved but uncharacterized domain (DUF3237, Figures 2A and S3). Crystal structures of

several members of the DUF3237 family have been elucidated to show a β -barrel fold (PDB entries 4PUX, 3G7G, and 3C5O), although no function is known (Figures S38 and S39). To determine the role of PhnH, we coexpressed PhnA, PhnB, PhnF, and PhnH in yeast, which led to the accumulation of a predominant new product **7** (Figure 2C-v). The structure of **7** was determined to be the known natural product atrovnetin^{17–19} (Figure S14) through extensive NMR analyses (Table S5 and Figures S22–S25). The absolute stereochemistry at C2' was assigned to be *R* by comparison of the optical rotation measurement ($[\alpha]_{\text{D}}^{26} = +90.5$ (*c* 0.02, MeOH)) to that reported for atrovnetin.²⁰ When purified **7** was added to the *phnA* blocked mutant, production of **2** was restored, verifying it is indeed an on-pathway product (Figure S4-iv). The 2' *R*-isomer of the autoxidized product **8** ($[\alpha]_{\text{D}}^{30} = +81.3$ (*c* 0.01, MeOH), Table S6 and Figures S26–S29) was also purified during isolation of **7** (Figure S15).

To demonstrate that PhnH is the sole enzyme required for the hydroalkoxylation reaction, PhnH was purified to homogeneity from yeast (Figure S6). A combined assay of PhnB, PhnF, and PhnH in the presence of **4** led to the formation of **7** as the predominant product (Figure 2D-iii). Direct incubation of **6a,b** with PhnH led to conversion to **7** (Figure 2D-iv–vii), with steady-state kinetic parameters of $k_{\text{cat}} = (2.9 \pm 0.3) \times 10^3 \text{ min}^{-1}$, $K_{\text{m}} = 216 \pm 19 \mu\text{M}$, and $k_{\text{cat}}/K_{\text{m}} = 13 \pm 1.4 \text{ min}^{-1} \mu\text{M}^{-1}$ (Figure S34B). Compared to the uncatalyzed reaction rate in DMSO ($k = 0.0086 \text{ min}^{-1}$, Figure S34A), PhnH afforded a $>3 \times 10^5$ -fold rate enhancement. Addition of 1 mM EDTA has no effect on the reaction rate (Figure S12), indicating no metal cofactor is required. The optimum pH for the enzyme is 7.5, as measured by the pH dependence assay, while nearly all activities are abolished when the pH is lowered to 6.0 (Figure S34C).

The stereochemical outcome of the hydroalkoxylation reaction catalyzed by PhnH is consistent with the isolation of 2' *R*-configured herqueinone **2** from *P. herquei*.²¹ The spontaneous, nonstereoselective formation of **7*** from **6** can also account for the isolation of the trace amounts 2' *S*-configured isoherqueinone.²² Identification of PhnH function also allowed us to complete the biosynthetic pathway of **2**. By sequentially adding remaining uncharacterized genes to the yeast host that produces **7**, we identified the *O*-methyltransferase PhnC as responsible for converting **7** to deoxyherqueinone **10** (Figure S4-vi).²³ The last C6 hydroxylation step that converts **10** to **2** was confirmed to be catalyzed by the FMO PhnG (Figure S4-vii). Hence, six enzymes are required to synthesize **2**, another example of the efficient biosynthetic pathways found in fungi.

We propose that PhnH catalyzes the hydroalkoxylation reaction by favoring binding of substrate **6a** in a near-attack conformation, thus aligning the lone electron pair of the deprotonated phenoxide anion in **6a'** (Figure 3A) with the Bürgi–Dunitz trajectory at the *S*-face of the C2'–C1' double bond. Concerted proton transfer from a nearby acid leads to protonation at C1' and yields product 2' *R*-**7**. Due to the extended aromatic system of **6**, the C7-phenol in **6a** is much more acidic, with $\text{p}K_{\text{a}} = 6.9$ (obtained from ACE JChem $\text{p}K_{\text{a}}$ predictor,²⁴ Figure S34D), indicating that no general base is required to generate the phenoxide anion of **6a'** at physiological pH (Figure 3A). Our DFT calculations show that acid catalysis likely occurs after the C7-OH is deprotonated, with an energy barrier of 21.8 kcal/mol using acetic acid as a general acid model (Figures 3B and S36A). Reaction

mechanisms that are not initiated by the deprotonation of C7-OH have been ruled out on the basis of calculations, due to either the high-energy barrier or unstable intermediates (Figures S36 and S37).

Proteins belonging to the DUF3237 superfamily are widely distributed in Nature, from bacteria to fungi, with many PhnH homologues embedded in potential natural product gene clusters (Figure S41). PhnH displays high sequence identity and homology to many members of the family (Figure S39). We generated a homology model of PhnH by using the I-TASSER server.²⁵ The model shows an overall β -barrel fold, typically adopted by the other members in the DUF3237 superfamily (Figure 3C). The model reveals a putative active site: a hydrophobic pocket with a Glu (E104) residue positioned at the bottom of the solvent-exposed cavity. Mutation at this residue compromised the enzymatic activity by ~60%. This indicates that E104, which may be deprotonated under assay conditions, is not a general acid but may be involved in properly positioning a water molecule (probably in its hydronium form) as a specific acid during the protonation reaction step. We also performed single-residue mutations at other conserved acidic positions based on sequence alignment. Different mutations led to varying degrees of attenuation in enzyme activity and expression levels, although no single mutation completely abolished PhnH activity (Table S8). Lastly, we synthesized 2-allyl resorcinol as a simplified substrate to test the promiscuity of PhnH. No rate acceleration of the hydroalkoxylation adduct was observed, which may be due to lack of recognition of the much smaller substrate by the enzyme and/or the significantly higher pK_a of the phenol group.

In conclusion, PhnH is the first functionally characterized protein member of the DUF3237 family. The discovery of PhnH complements other enzymatic strategies to synthesize cyclic ethers in natural products.^{1a,26} Therefore, PhnH provides an enzymatic variant of asymmetric hydroalkoxylation of olefins, an important transformation in synthetic chemistry.

Supplementary Material

Refer to Web version on PubMed Central for supplementary material.

Acknowledgments

This work was supported by the NIH (1DP1GM106413 and 1R35GM118056 to Y.T.), the NSF (CHE-1361104 to K.N.H.), and the Chemistry–Biology Interface training program (NRSA 5T32GM008496-20 to J.S.B.). M.G.-B. thanks the Ramón Areces Foundation for a Postdoctoral Fellowship.

References

1. (a) Hemmerling F, Hahn F, Beilstein J Org Chem. 2016; 12:1512. [PubMed: 27559404] (b) Taylor RD, MacCoss M, Lawson ADG. J Med Chem. 2014; 57:5845. [PubMed: 24471928]
2. (a) Thomas CM, Hothersall J, Willis CL, Simpson T. Nat Rev Microbiol. 2010; 8:281. [PubMed: 20190824] (b) Okouneva T, Azarenko O, Wilson L, Littlefield BA, Jordan MA. Mol Cancer Ther. 2008; 7:2003. [PubMed: 18645010] (c) Finkelstein E, Amichai B, Grunwald MH. Int J Antimicrob Agents. 1996; 6:189. [PubMed: 18611708]
3. Sheppard TD. J Chem Res. 2011; 35:377.
4. Beller M, Seayad J, Tillack A, Jiao H. Angew Chem, Int Ed. 2004; 43:3368.

5. Smith, MB., March, J. *March's Advanced Organic Chemistry*. John Wiley & Sons, Inc; New York: 2006. p. 1251
6. (a) Rosenfeld DC, Shekhar S, Takemiya A, Utsunomiya M, Hartwig JF. *Org Lett*. 2006; 8:4179. [PubMed: 16956181] (b) Jeong Y, Kim DY, Choi Y, Ryu JS. *Org Biomol Chem*. 2011; 9:374. [PubMed: 21076772]
7. For select examples of transition-metal-catalyzed hydroalkoxylation, see: Hay MB, Hardin AR, Wolfe JP. *J Org Chem*. 2005; 70:3099. [PubMed: 15822970] Zhang Z, Widenhoefer RA. *Angew Chem, Int Ed*. 2007; 46:283. Murayama H, Nagao K, Ohmiya H, Sawamura M. *Org Lett*. 2015; 17:2039. [PubMed: 25849322] Schlüter J, Blazejak M, Boeck F, Hintermann L. *Angew Chem, Int Ed*. 2015; 54:4014. Liu Z, Breit B. *Angew Chem, Int Ed*. 2016; 55:8440. Li J, Lin L, Hu B, Zhou P, Huang T, Liu X, Feng X. *Angew Chem, Int Ed*. 2017; 56:885. Hack D, Chauhan P, Deckers K, Mizutani Y, Raabe G, Enders D. *Chem Commun*. 2015; 51:2266.
8. (a) Wise ML, Savage TJ, Katahira E, Croteau R. *J Biol Chem*. 1998; 273:14891. [PubMed: 9614092] (b) Piechulla B, Bartelt R, Brosemann A, Effmert U, Bouwmeester H, Hippauf F, Brandt W. *Plant Physiol*. 2016; 172:2120. [PubMed: 27729471] (c) Wise ML, Urbansky M, Helms GL, Coates RM, Croteau R. *J Am Chem Soc*. 2002; 124:8546. [PubMed: 12121093]
9. Kalaitzis JA, Hamano Y, Nilsen G, Moore BS. *Org Lett*. 2003; 5:4449. [PubMed: 14602022]
10. Brooks JS, Morrison GA. *J Chem Soc, Perkin Trans 1*. 1972:421.
11. Fun HK, Chantrapromma S, Boonnak N, Karalai C, Chantrapromma K. *Acta Crystallogr, Sect E*. 2011; 67:o1916.
12. Gao SS, Duan A, Xu W, Yu P, Hang L, Houk KN, Tang Y. *J Am Chem Soc*. 2016; 138:4249. [PubMed: 26978228]
13. Elsebai MF, Saleem M, Tejesvi MV, Kajula M, Mattila S, Mehiri M, Turpeinen A, Pirttila AM. *Nat Prod Rep*. 2014; 31:628. [PubMed: 24686921]
14. McIntosh JA, Donia MS, Nair SK, Schmidt EW. *J Am Chem Soc*. 2011; 133:13698. [PubMed: 21766822]
15. Hao Y, Pierce E, Roe D, Morita M, McIntosh JA, Agarwal V, Cheatham TE, Schmidt EW, Nair SK. *Proc Natl Acad Sci U S A*. 2016; 113:14037. [PubMed: 27872314]
16. Rudolf JD, Poulter CD. *ACS Chem Biol*. 2013; 8:2707. [PubMed: 24083562]
17. Ayer WA, Hoyano Y, Pedras MS, Clardy J, Arnold E. *Can J Chem*. 1987; 65:748.
18. Ishikawa Y, Morimoto K, Iseki S. *J Am Oil Chem Soc*. 1991; 68:666.
19. Paul IC, Sim GA. *J Chem Soc*. 1965:1097. [PubMed: 14267229]
20. Neill KG, Raistrick H. *Biochem J*. 1957; 65:166. [PubMed: 13403888]
21. (a) Tansakul C, Rukachaisirikul V, Maha A, Kongprapan T, Phongpaichit S, Hutadilok-Towatana N, Borwornwiriyanon K, Sakayaroj J. *Nat Prod Res*. 2014; 28:1718. [PubMed: 25079041] (b) Quick A, Thomas R, Williams DJ. *J Chem Soc, Chem Commun*. 1980:1051.
22. Brooks JS, Morrison GA. *Tetrahedron Lett*. 1970; 11:963.
23. Barton DHR, de Mayo P, Morrison GA, Raistrick H. *Tetrahedron*. 1959; 6:48.
24. ACE and JChem acidity and basicity calculator. 2016. <https://epoch.uky.edu/ace/public/pKa.jsp>
25. Zhang Y. *BMC Bioinf*. 2008; 9:40.
26. Tang MC, Zou Y, Watanabe K, Walsh CT, Tang Y. *Chem Rev*. 2017; doi: 10.1021/acs.chemrev.6b00478

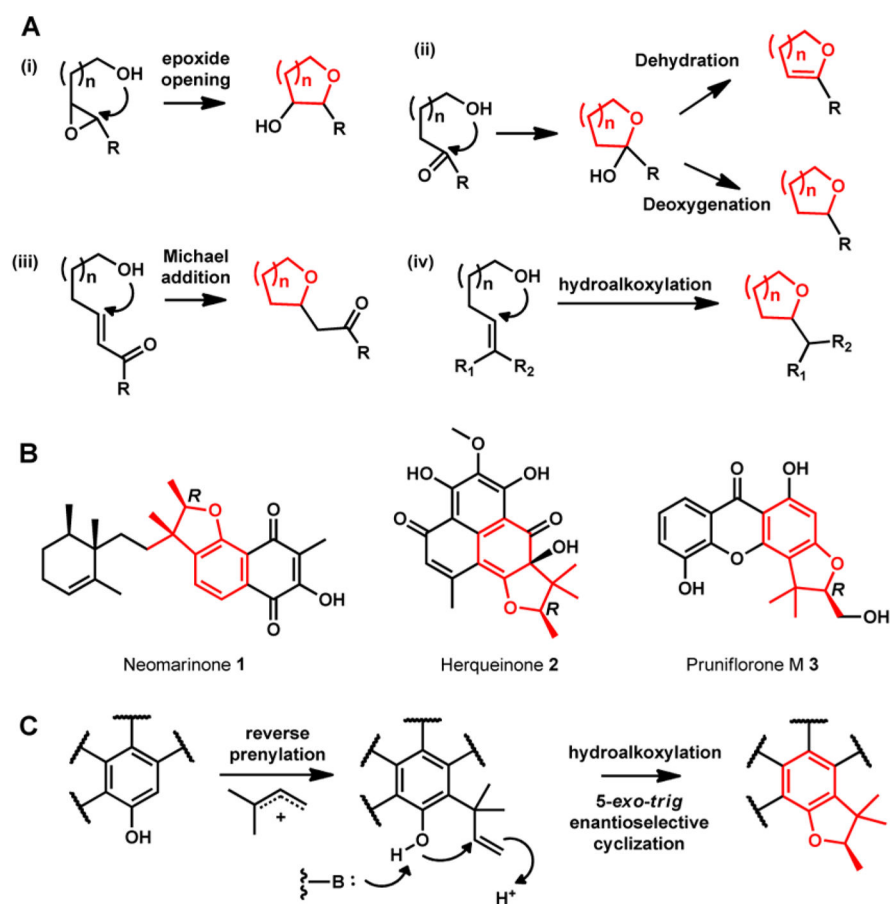


Figure 1. (A) Routes to generate cyclic ethers. (B) Natural products containing 2,3,3-trisubstituted DHF moiety from bacteria (1), fungi (2), and plants (3). See Figure S2 for more examples. (C) Proposed cyclization steps required for the formation of 2,3,3-trisubstituted DHF moiety. Reverse prenylation is followed by intramolecular hydroalkoxylation under general acid and general base catalysis.

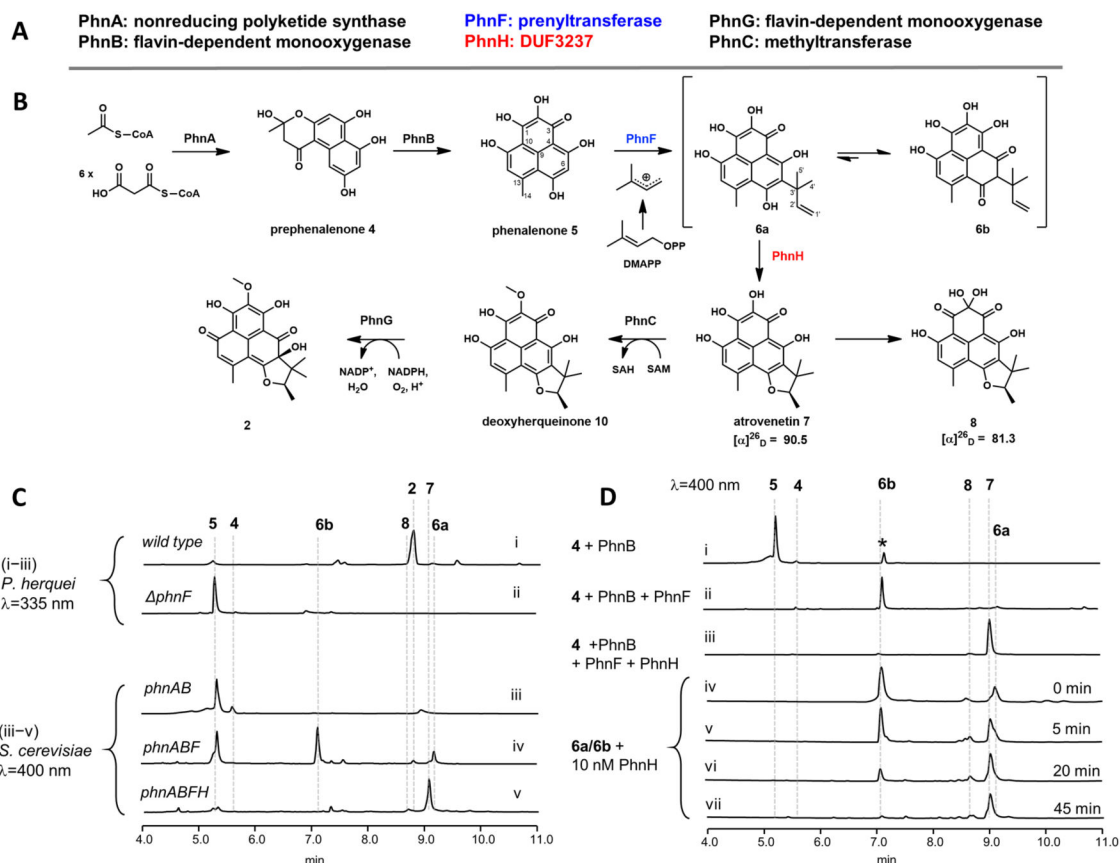
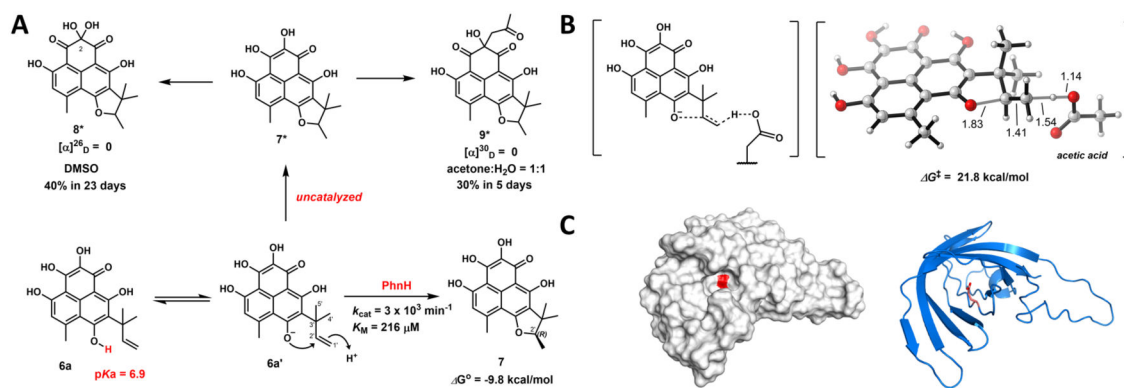


Figure 2. Characterization of the herqueinone **2** pathway. (A) Key enzymes encoded in the *phn* cluster. (B) Complete biosynthetic pathway of **2**. (C) Product profiles of wild-type and *phnF* knockout mutant of *P. herquei* and of *S. cerevisiae* transformed with combinations of *phn* genes. (D) Product profiles of in vitro assays using purified enzymes. *The spontaneous degradative product of **5**.¹² See SI for reaction conditions.

**Figure 3.**

(A) Proposed mechanism for PhnH-catalyzed hydroalkoxylation. PhnH catalyzes *5-exo-trig* cyclization via acid catalysis after the spontaneous deprotonation of 7-OH. (B) Transition-state structure of the hydroalkoxylation reaction using acetic acid as a general acid. (C) Homology models of PhnH. The putative catalytic residue E104 is highlighted in red.